

1 **Germline and somatic genetic variants in the p53 pathway interact to affect cancer risk,**
2 **progression, and drug response**

3 Running title: p53 pathway SNPs and mutations interact to affect cancer

4 Ping Zhang^{1,18}, Isaac Kitchen-Smith¹, Lingyun Xiong¹, Giovanni Stracquadanio^{1,16}, Katherine Brown^{2,17}, Philipp H.
5 Richter¹, Marsha D. Wallace^{1,18}, Elisabeth Bond¹, Natasha Sahgal¹, Samantha Moore¹, Svanhild Nornes^{1,20}, Sarah De
6 Val^{1,20}, Mirvat Surakhy¹, David Sims², Xuting Wang³, Douglas A. Bell³, Jorge Zeron-Medina^{1,15}, Yanyan Jiang⁴,
7 Anderson J. Ryan⁴, Joanna L. Selfe⁵, Janet Shipley⁵, Siddhartha Kar^{6,19}, Paul D. Pharoah⁶, Chey Loveday⁷, Rick Jansen⁸,
8 Lukasz F. Grochola⁹, Claire Palles¹⁰, Andrew Protheroe¹², Val Millar¹³, Daniel V. Ebner¹³, Meghana Pagadala¹⁴, Sarah P.
9 Blagden¹¹, Timothy S. Maughan¹¹, Enric Domingo¹¹, Ian Tomlinson¹⁰, Clare Turnbull⁷, Hannah Carter¹⁴ and Gareth L.
10 Bond^{1,21}

11 ¹Ludwig Institute for Cancer Research, University of Oxford, Nuffield Department of Clinical Medicine, Old Road
12 Campus Research Building, Oxford OX3 7DQ, UK

13 ²Weatherall Institute of Molecular Medicine, University of Oxford, John Radcliffe Hospital, Oxford OX3 9DS, UK

14 ³Environmental Epigenomics and Disease Group, Immunity, Inflammation, and Disease Laboratory, National Institute of
15 Environmental Health Sciences-National Institutes of Health, Research Triangle Park, NC 27709, USA

16 ⁴CRUK & MRC Oxford Institute for Radiation Oncology, University of Oxford, Department of Oncology, Old Road
17 Campus Research Building, Oxford OX3 7DQ, UK

18 ⁵Sarcoma Molecular Pathology Team, Divisions of Molecular Pathology and Cancer Therapeutics, The Institute of
19 Cancer Research, Sutton, Surrey SM2 5NG, UK.

20 ⁶Department of Public Health and Primary Care, University of Cambridge, Cambridge CB1 8RN, UK

21 ⁷Division of Genetics and Epidemiology, The Institute of Cancer Research, London SW3 6JB, UK

22 ⁸Amsterdam UMC, Vrije Universiteit Amsterdam, Department of Psychiatry, Amsterdam Neuroscience, the Netherlands

23 ⁹Department of Surgery, Cantonal Hospital Winterthur, Switzerland

24 ¹⁰Institute of Cancer and Genomic Sciences, University of Birmingham, Birmingham B15 2TT, UK

25 ¹¹Department of Oncology, University of Oxford, Oxford OX3 7DQ, UK

26 ¹²Oxford Cancer and Haematology Centre, Oxford University Hospitals NHS Foundation Trust, Oxford OX3 7LE, UK.

27 ¹³Target Discovery Institute, University of Oxford, Nuffield Department of Medicine, Oxford OX3 7FZ, UK

28 ¹⁴Department of Medicine, University of California, San Diego, La Jolla, CA 92093, USA

29

30 ¹⁵Current address: Translational Medicine, Research and Early Development, Oncology R&D, AstraZeneca, Waltham,
31 Massachusetts, USA

32 ¹⁶Current address: Institute of Quantitative Biology, Biochemistry, and Biotechnology, SynthSys, School of Biological
33 Sciences, University of Edinburgh, Edinburgh, UK

34 ¹⁷Current address: Division of Virology, Department of Pathology, University of Cambridge, Cambridge, UK

35 ¹⁸Current address: Wellcome Centre for Human Genetics, University of Oxford, Oxford, UK

36 ¹⁹Current address: MRC Integrative Epidemiology Unit, Population Health Sciences, Bristol Medical School, University
37 of Bristol, UK

38 ²⁰Current address: Department of Physiology, Anatomy and Genetics, University of Oxford, UK

39 ²¹Current address: Institute of Cancer and Genomic Sciences, University of Birmingham, Birmingham B15 2TT, UK

40

41 **Corresponding Authors:**

42 Hannah Carter, UCSD, 9500 Gilman Drive, La Jolla, CA 92093-0688. Phone: 858-822-4706; Fax: 858-822-4246; E-
43 mail: hkcarter@health.ucsd.edu;

44 Gareth L. Bond, Institute of Cancer and Genomic Sciences, University of Birmingham, B15 2TT, United Kingdom.
45 Phone: 0044-(0)121 414 3344; E-mail: G.Bond.1@bham.ac.uk

46

47 **Declaration of Interests**

48 The authors declare no competing interests.

49

50 **Abstract**

51 Insights into oncogenesis derived from cancer susceptibility loci (single nucleotide polymorphisms,
52 SNP) hold the potential to facilitate better cancer management and treatment through precision
53 oncology. However, therapeutic insights have thus far been limited by our current lack of
54 understanding regarding both interactions of these loci with somatic cancer driver mutations and
55 their influence on tumorigenesis. For example, while both germline and somatic genetic variation to
56 the p53 tumor suppressor pathway are known to promote tumorigenesis, little is known about the
57 extent to which such variants cooperate to alter pathway activity. Here we hypothesize that cancer
58 risk-associated germline variants interact with somatic *TP53* mutational status to modify cancer risk,
59 progression, and response to therapy. Focusing on a cancer risk SNP (rs78378222) with a well-
60 documented ability to directly influence p53 activity as well as integration of germline datasets
61 relating to cancer susceptibility with tumor data capturing somatically-acquired genetic variation
62 provided supportive evidence for this hypothesis. Integration of germline and somatic genetic data
63 enabled identification of a novel entry point for therapeutic manipulation of p53 activities. A cluster
64 of cancer risk SNPs resulted in increased expression of pro-survival p53 target gene *KITLG* and
65 attenuation of p53-mediated responses to genotoxic therapies, which were reversed by
66 pharmacological inhibition of the pro-survival c-KIT signal. Together, our results offer evidence of
67 how cancer susceptibility SNPs can interact with cancer driver genes to affect cancer progression
68 and identify novel combinatorial therapies.

69

70 **Significance**

71 These results offer evidence of how cancer susceptibility SNPs can interact with cancer driver genes
72 to affect cancer progression and present novel therapeutic targets.

73 **Introduction**

74 Efforts to characterize the somatic alterations that drive oncogenesis have led to the
75 development of targeted therapies, facilitating precision approaches that condition treatment on
76 knowledge of the tumor genome, and improving outcomes for many cancer patients (1,2). However,
77 such targeted therapies are associated with variable responses, eventual high failure rates and the
78 development of drug resistance. Somatic genetic heterogeneity among tumors is a major factor
79 contributing to differences in disease progression and therapeutic response (1). Inter-individual
80 differences may arise not only from different somatic alterations, but also from differences in the
81 underlying genetic background. The maps of common germline genetic variants that associate with
82 disease susceptibility allow us to generate and test biological hypotheses, characterize regulatory
83 mechanisms by which variants contribute to disease, with the aim of integrating the results into the
84 clinic. However, there are challenges in harnessing susceptibility loci for target identification for
85 cancer, including limitations in (i) exposition of causative variants within susceptibility loci, (ii)
86 understanding of interactions of susceptibility variants with somatic driver mutations, and (iii)
87 mechanistic insights into their influence on cellular behaviors during and after the evolution of
88 somatic cancer genomes (3-5).

89 A key cancer signaling pathway known to harbor multiple germline and somatic variants
90 associated with cancer susceptibility is the p53 tumor suppressor pathway (6). It is a stress response
91 pathway that maintains genomic integrity and is among the most commonly perturbed pathways in
92 cancer, with somatic driver mutations found in the *TP53* gene in more than 50% of cancer genomes
93 (7). Loss of the pathway and/or the gain of pro-cancer mutations can lead to cellular transformation
94 and tumorigenesis (8). Once cancer has developed, the p53 pathway is important in mediating cancer
95 progression and the response to therapy, as its anti-cancer activities can be activated by many
96 genotoxic anticancer drugs (9). These drugs are more effective in killing cancers with wild-type p53
97 relative to mutant p53 (10,11). While both germline and somatic alterations to the p53 pathway are
98 known to promote tumorigenesis, the extent to which such variants cooperate to alter pathway
99 activity and the effects on response to therapy remain poorly understood.

100 Most studies have separately examined the consequences of somatic and germline variation
101 affecting p53 activity to understand their roles in disease risk, progression or response to therapy.
102 Here we hypothesize that cancer-associated germline variants (single nucleotide polymorphisms,
103 SNPs) interact with *TP53* somatic driver mutations to modify cancer risk, progression and potential
104 to respond to therapy. With a focus on a cancer-associated SNP that directly influences p53 activity,

105 we provide supportive evidence for this hypothesis, and go on to demonstrate how such germline-
106 somatic interactions inform discovery of candidate drug targets.

107

108 **Materials and Methods**

109 **Assigning *TP53* mutational status to breast, ovarian cancers and TCGA tumors**

110 We curated *TP53* pathogenic missense mutations by integrating up-to-date functional evidence from
111 both literature and databases as detailed in Supplementary Information. In total, we were able to find
112 218 out of 323 *TP53* pathogenic mutations are oncogenic (**Supplementary Table S1**). All *TP53*
113 missense mutations in breast, ovarian cancers and TCGA primary tumors were extracted and
114 matched with the curated lists of pathogenic and oncogenic *TP53* missense mutations.

115

116 **Analysis for subtype heterogeneity SNPs with Breast and Ovarian cancer association studies**

117 Estimates of effect sizes [$\log(\text{OR})$ s] for subtype-specific case-control studies and their corresponding
118 standard errors were utilized for meta- and heterogeneity-analyses using METAL (2011-03-25
119 release) (12), under an inverse variance fixed-effect model. See Supplementary Information for
120 details.

121

122 **Cancer GWAS SNPs**

123 We selected the GWAS significant lead SNPs (p -value $<5e-08$) in Europeans, and retrieved the
124 associated proxy SNPs using the 1000 Genomes phase 3 data through the web server rAggr. See
125 Supplementary Information for details.

126

127 **Enrichment analysis**

128 The hypergeometric distribution enrichment analysis was performed as described in (6). Significance
129 was determined using PHYPHER function as implemented in R and multiple hypotheses testing by
130 Benjamini-Hochberg correction.

131

132 **Genotype imputation and population stratification**

133 Genotype data was obtained and filtered as described in (3). The genotype data of 7,021 TCGA
134 patients were clustered tightly with Europeans. See Supplementary Information for details.

135

136 **TCGA survival analysis**

137 The omics datasets (gene mutation, copy number and mRNA expression) of the TCGA cohort were
138 downloaded from the cBioPortal (<https://www.cbioportal.org/>). We considered those mutations with
139 putative oncogenic properties (marked as 'Oncogenic', 'Likely Oncogenic' or 'Predicted Oncogenic'
140 in OncoKB) as oncogenic mutations. TCGA clinical data was downloaded from the recently updated
141 Pan-Cancer Clinical Data Resource (TCGA-CDR) (13). TCGA clinical radiation data was retrieved
142 using R package TCGAbiolinks (V2.16.1). The patients with "Radiographic Progressive Disease"
143 were defined as radiation non-responders. Patients with "Complete Response" or "Partial Response"
144 were defined as responders. A Cox proportional hazards regression model was used to calculate the
145 hazard ratio, the 95% confidence interval and p values for the two-group comparisons. The log-rank
146 test was used to compare the differences of Kaplan-Meier survival curves. The clinical, gene
147 expression and mutation data for the DFCI-SKCM cohort was downloaded from cBioPortal. The
148 optimal cut-off of the gene expression for the survival analysis was determined using the
149 survcutpoint function of the survminer R package, and used to stratify the patients into high- and
150 low-risk groups.

151

152 **GDSC drug sensitivity analysis**

153 *TP53* mutation, copy number, RNAseq gene expression data, and drug IC50 values for the cancer
154 cell lines were downloaded from Genomics of Drug Sensitivity in Cancer (GDSC; release-8.1). The
155 classified cell lines based on *TP53* mutational status were further grouped based on the gene
156 transcript levels: low (\leq 1st quartile), intermediate ($>$ 1st quartile and $<$ 3rd quartile), high (\geq 3rd
157 quartile). The effects of the mutation status or transcript levels on drug sensitivity were then
158 determined with a linear model approach. See details in Supplementary Information.

159

160 **Cell culture and their treatments**

161 Testicular cancer cell lines TERA1, TERA2, 2102EP, Susa-CR, GH, were cultured in RPMI medium
162 containing 10% fetal bovine serum and 1% penicillin/streptomycin according to standard conditions.
163 Susa cells were cultured in RPMI medium containing 20% fetal bovine and 1%

164 penicillin/streptomycin. GCT27 and GCT27-CR were cultured in DMEM supplemented with 10%
165 fetal bovine serum and 1% penicillin/streptomycin. Hap1 cells were obtained from Horizon
166 Discovery Ltd and cultured in IMDM (Sigma-Aldrich Co Ltd) supplemented with 10% fetal bovine
167 serum and 1% penicillin/streptomycin. FuGENE 6 Transfection Reagent (Promega) was used for
168 DNA transfection. For transfection of siRNA, Lipofectamine RNAiMAX Transfection Reagent
169 (ThermoFisher) was used. The cell lines were tested for Mycoplasma contamination every 3-4 weeks
170 using MycoAlert™ mycoplasma detection kit (Lonza), and used for experiments at less than 20
171 passages. Cell line authentication was performed by STR (Short Tandem Repeat) analysis (Eurofins
172 Genomics).

173

174 **CRISPR/Cas9-mediated genome editing**

175 The Cas9 expression vector was obtained from Addgene (#62988). sgRNAs were designed and
176 constructed as described previously (14). The oligo sequences for the sgRNA synthesis are listed in
177 **Supplementary Table S2**. See Supplementary Information for details.

178

179 **RNA isolation, qRT-PCR and RNA-seq analysis**

180 RNA isolation, qRT-PCR and RNA-seq analysis were performed as detailed in Supplementary
181 Information.

182

183 **Drug screening**

184 Cells were seeded in 384-well plates (flat bottom, black with clear bottom, Greiner) at density of
185 about 2,000 cells per well in 81µl with cell dispenser (PerkinElmer) and liquid handling robotics
186 (JANUS, PerkinElmer) and incubated overnight. Next, library compounds (**Supplementary Table**
187 **S3**) were added to a final concentration of 10µM, 1µM, 100nM or 10nM. Dasatinib (1µM) was
188 added as positive control and DMSO (Vehicle, 0.1%) was added as negative control. After 72 hours,
189 cell were fixed with 4% paraformaldehyde for 10 min, permeabilized with 0.5% Triton X-100 for 5
190 min, and then stained with 1:1000 dilution of 5mg/ml DAPI for 5 min. Next, the plates were imaged
191 using a high-content analysis system (Operetta, PerkinElmer). The image data was analyzed by an
192 image data storage and analysis system (Columbus, PerkinElmer). The cells with nuclear area>150
193 and nuclear intensity<700 were counted, and cell number was used as the viability readout. The
194 screen was performed in duplicate. The Pearson Correlation Coefficient, a measurement for inter-

195 assay variability, averaged 0.98 and an average Z-factor, a measure employed in high throughput
196 screens to measure effect size, of 0.69 for all plates was recorded, leading to high confidence in the
197 primary screen positive hits (**Supplementary Table S4**).

198

199 **SDS-PAGE and western blotting**

200 SDS-PAGE and western blotting was performed as described in (15). The antibodies against p53 (sc-
201 126), c-KIT (sc-17806), PARP1 (sc-7150), and β -Actin (sc-47778) were from Santa Cruz (Dallas,
202 TX, USA). The antibodies against acetylated p53 (Lys382, #2525), cleaved Caspase 3 (Asp175,
203 #9661) were from Cell Signaling. HRP-coupled secondary antibodies were from Dako.

204

205 **IC50 and combination index CI analyses**

206 To determine an IC50, 8 multiply diluted concentrations were used including a PBS control for 48
207 hour treatments and then cell viability was assessed by a MTT assay (see details in Supplementary
208 Information). The IC50 was calculated using the Graphpad Prism software. A constant ratio matrix
209 approach was used to determine the combination index CI values (16). Single drug data and
210 combination data was entered into Compusyn software (<http://www.combosyn.com>) to compute
211 CI50 and dose-reduction index (DRI). CI50 is $(CX/IC50(X)) + (CY/IC50(Y))$, where $(CX/IC50(X))$
212 is the ratio of the drug X's concentration (CX) in a 50% effective drug mixture to its 50% inhibitory
213 concentration (IC50(X)) when applied alone. The CI50 values quantitatively depict synergistic
214 ($CI < 1$), additive ($CI = 1$), and antagonistic effects ($CI > 1$).

215

216 ***In vivo* study**

217 All animal procedures were carried out under a UK Home Office project licence (PPL30/3395).
218 Before submitting to the Home Office, the project licence was approved by the Oxford University
219 Animal Welfare and Ethical Review Board (AWERB). Mice were housed at Oxford University
220 Biomedical Services, UK. 6-8 week-old female BALB/c nude mice (Charles River, UK) were
221 injected subcutaneously. See Supplementary Information for details.

222

223 **Results**

224 **1. p53 regulatory cancer risk SNP rs78378222 associates with subtype heterogeneity**

225 To represent germline effects, we focused on the cancer risk-associated SNP with the most
226 direct and most understood influence on p53 activity. This SNP, rs78378222, resides in the 3'-UTR
227 in the canonical *TP53* polyadenylation signal (p53 poly(A) SNP). The minor C-allele is known to
228 associate with lower *TP53* mRNA levels in different normal tissue types, such as in blood, skin,
229 adipose, esophagus-mucosa, and fibroblasts (17,18), and associate strongly with differential risk of
230 many cancer types (19-23).

231 We explored whether the p53 poly(A) SNP can differentially influence mutant and wild-type
232 *TP53* (*wtTP53*) cancer risk by studying cancers with subtypes that differ substantially in *TP53*
233 mutation frequencies and for which susceptibility GWAS data are available. 18% of estrogen
234 receptor positive breast cancers (ER+BC) mutate *TP53*, in contrast to 76% of estrogen receptor
235 negative breast cancers (ER-BC) (24). Similarly, less than 10% of low-grade serous ovarian cancers
236 (LGSOC) mutate *TP53*, in contrast to 96% of high grade serous ovarian cancers (HGSOC) (25).
237 Over 85% of *TP53* pathogenic missense mutations in breast and ovarian cancers are oncogenic
238 (either dominant negative or gain-of-function) (**Fig. 1A**) (see Methods). We analyzed data from
239 90,969 breast cancer patients of European ancestry (69,501 ER-pos BC, 21,468 ER-neg BC) (26)
240 and 105,974 controls, and 14,049 ovarian cancer patients of European ancestry (1,012 LGSOC,
241 13,037 HGSOC) and 40,941 controls (27).

242 It is known that key regulatory pathway genes and stress signals, which can regulate *wtTP53*
243 levels and tumor suppressive activities, can also regulate mutant p53, including its oncogenic
244 activities (28,29). Thus, if the poly(A) SNP can influence both mutant and *wtTP53* expression, the
245 minor C-allele (less *TP53* expression) would be expected to have opposite associations with disease
246 subtype (**Fig. 1B**). That is, the minor C-allele would associate with increased cancer risk ($OR > 1$) in
247 the subtypes with low *TP53* mutation frequencies (ER+BC and LGSOC), and decreased cancer risk
248 ($OR < 1$) in the subtypes with high *TP53* mutation frequencies (ER-BC and HGSOC). Indeed, this is
249 the case, whereby we found an increase in the frequency of the minor C-allele in ER+BC and
250 LGSOC patients compared to healthy controls ($OR = 1.12$, $p = 1.0e-03$ and $OR = 1.59$, $p = 0.016$,
251 respectively) (**Fig. 1C**), but a decreased frequency in ER-BC and HGSOC patients compared to
252 controls ($OR = 0.80$, $p = 2.3e-04$ and $OR = 0.75$, $p = 3.7e-04$, respectively). Taken together, the
253 distribution of minor C-allele shows significant heterogeneity among the four cancer subtypes (p -
254 $het = 2.59e-09$).

255 The above analysis supports a persistent effect for the p53 cancer risk SNP on tumors through a
256 possible influence on whether or not a tumor contains a somatically mutated *TP53* locus. In order to
257 seek further and more direct support of this possibility, we performed similar analyses of the p53

258 poly(A) SNP in a cohort of 7,021 patients of European origin diagnosed with 31 different cancers
259 and for whom the *TP53* mutational status of their cancers could be determined (The Cancer Genome
260 Atlas, TCGA). We partitioned the patients into two groups based on the presence or absence of the
261 *TP53* somatic alteration (mutation and CNV loss versus WT and no CNV loss; (**Fig. 1D**).

262 Interestingly, the p53 poly(A) SNP associated with allelic differences in minor allele frequencies
263 between the groups of patients with either *wtTP53* or mutant tumors (**Fig. 1E**). This is in line with
264 the associations found with *TP53* mutational status of breast and ovarian cancer subtypes, whereby
265 the C-allele is more frequent in *wtTP53* tumors.

266 **2. A p53 regulatory cancer risk SNP can affect wild type and mutant *TP53* in tumors, and** 267 **associates with clinical outcomes.**

268 As mentioned above, the minor C-allele of the p53 poly(A) SNP has been previously found to
269 associate with lower p53 mRNA levels in many different normal tissues and cells (18). To
270 investigate the activity of this SNP in tumors, we analyzed expression data from 3,248 tumors from
271 the TCGA cohort, for which both germline and somatic genetic data are available and no somatic
272 copy number variation of *TP53* could be detected. Similar to results obtained in the normal tissues,
273 we observed a significant association of the minor C-allele with lower *TP53* expression levels in the
274 tumors, estimated 1.5-fold per allele ($p=1.7e-04$, $\beta=-0.37$; **Fig. 2A**). To test if the C-allele
275 associates with lower levels of both wild type and mutant *TP53*, we divided the tumors into three
276 groups based on their respective somatic *TP53* mutational status (**Supplementary Fig. 1A** and
277 **Supplementary Table S5**). We found 2,521 tumors with *wtTP53*, 448 with missense mutations, and,
278 of those, 389 with oncogenic missense mutations. In all three groups, the C-allele significantly
279 associates with lower *TP53* expression levels (**Supplementary Fig. 1B**).

280 Next, we utilized Hap1 cells that contain a dominant-negative *TP53* missense mutation
281 (p.S215G), which results in a mutated DNA-binding domain (30). We generated clones with either
282 the A-allele or the C-allele (**Fig. 2B**), and found significantly lower *TP53* mRNA levels in cells with
283 the C-allele relative to the A-allele (~2 fold, **Fig. 2C**). We also found the C-allele containing cells
284 express less p53 protein (**Supplementary Fig. 1C**). The impairment of 3'-end processing and
285 subsequent transcription termination by the minor allele of the p53 poly(A) SNP, have been
286 proposed as a mechanism for the genotype-dependent regulatory effects on *TP53* expression (17).
287 Indeed, we observed significant enrichments of uncleaved *TP53* mRNA in cells carrying the C-allele
288 compared to the A-allele by qRT-PCR and 3' RNA-sequencing (**Supplementary Fig. 1D-E**).
289 Together, our data demonstrate that this cancer risk-associated SNP can influence the expression of
290 both wild type and mutant *TP53* in cancer cells and tumors.

291 To explore whether the p53 poly(A) SNP also associates with allelic differences in clinical
292 outcomes, we stratified the TCGA cohort into two groups based on *TP53* somatic alterations and the
293 p53 poly(A) SNP genotypes. We found that in patients with *wtTP53* tumors, those with the minor C-
294 alleles have a significantly shorter PFI and worse OS compared to those without the minor alleles
295 (**Fig. 2D**), but not in patients without stratification. An inverted, but not significant trend, among the
296 patients with somatic *TP53* mutations is noted. Similarly, significant, *TP53* mutational status-
297 dependent, associations between the p53 poly(A) SNP and PFI can be found when we restrict our
298 analyses to breast cancer patients only (**Fig. 2E**).

299 It is well documented that p53 somatic mutations antagonise cellular sensitivity to radiotherapy
300 (31), an important component of current cancer treatments. Indeed, we see not only *TP53* mutations,
301 but also the p53 poly(A) SNP play roles in the radiation response phenotype in the TCGA cohort.
302 Specifically, we focused on the 7021 patients for whom the SNP genotypes were available. Of these,
303 848 patients could be assigned with radiation response phenotypes (603 responders; 134 non-
304 responders; see Methods). We determined that the radiation non-responders were significantly
305 enriched in patients with *TP53* somatic mutations (OR= 1.6, $p = 0.021$; **Fig. 2F**). The enrichment
306 was further enhanced when we analysed those patients with both *TP53* mutations and copy number
307 loss (OR = 2.2, $p = 0.0026$). Importantly, we also found that in patients with *wtTP53* tumors, but not
308 with *TP53* mutant tumors, radiation non-responders were greatly enriched in the C-allele of the p53
309 poly(A) SNP (less *TP53* expression (OR = 5.6, $p = 0.011$ for risk allele; **Fig. 2F**).

310 **3. Somatic copy number loss of *TP53* can mimic effects of the p53 poly(A) SNP**

311 Together, the results we have presented thus-far suggest that the relative 2-fold reduction of
312 *wtTP53* levels in tumors from patients with the minor allele of the p53 regulatory SNP can lead to
313 worse clinical outcomes and treatment response. If true, we reasoned that we should be able to find
314 similar associations in patients whose tumors lose a single copy of *TP53*. In the TCGA database,
315 1839 (26.6%) patients with *wtTP53* tumors, and 2236 (59.3%) patients with mutant *TP53* tumors
316 show significant signs of loss at the *TP53* locus (estimated one copy on average, GISTIC score -1).
317 These tumors associate with 1.3-fold and 1.1-fold lower *TP53* RNA expression respectively
318 compared to the tumors without loss (**Fig. 2G**). In support of small reductions of *TP53* expression
319 affecting patient outcome, we found that *wtTP53*-loss associates with shorter PFI and worse OS
320 compared to no *wtTP53*-losses (**Fig. 2H**), but are not found in patients with mutant *TP53*. These
321 associations are independent of tumor type (adjusted $p < 0.05$; **Fig. 2H**). We also found in patients
322 with *wtTP53* tumors, that radiotherapy non-responders are significantly enriched in cancers with
323 *TP53* copy number loss (OR =1.6, $p = 0.027$; **Fig. 2I**).

324 We next sought to test whether the modest changes in *TP53* expression (<2 fold) could predict
325 chemosensitivities. We used the drug sensitivity dataset with both somatic genetic and gene
326 expression data (GDSC; 304 drugs across 987 cell lines). Similar to what we observed in TCGA
327 tumors, *TP53* copy number loss in cancer cell lines associates with a modest reduction in *TP53*
328 expression (**Fig. 3A**). Strikingly, and as predicted, *wtTP53* loss, but not mutant *TP53*-loss,
329 significantly associates with reduced sensitivities to 31% of the drugs tested (**Fig. 3B**;
330 **Supplementary Table S6**). Specifically, 93 out of the 304 drugs demonstrated reduced sensitivity in
331 *wtTP53* cell lines with *TP53*-loss compared to those without a loss (adjusted $p < 0.05$; **Fig. 3B**).
332 These drugs included many known p53 activating agents including an MDM2 inhibitor (Nutlin3), as
333 well as standard chemotherapeutics such as cisplatin, doxorubicin, and etoposide. Together, our
334 observations clearly indicate that patients whose tumors have modest decreases in *wtTP53*
335 expression, mediated either through the regulatory SNP or somatic *TP53* copy number loss, associate
336 with poorer DNA-damage responses and clinical outcomes.

337 **4. A drug-able p53 pathway gene with cancer risk SNPs associates with pathway inhibitory** 338 **traits**

339 Various therapeutic efforts have been designed around restoring wild-type p53 activity to
340 improve p53-mediated cell killing (32). The identification of a p53 regulatory cancer risk SNP that
341 affects, in tumors, *TP53* expression levels, activity, *TP53* mutational status, tumor progression,
342 outcome and radiation responses (as demonstrated for the p53 poly(A) SNP) points to other potential
343 entry points for therapeutically manipulating p53 activities guided by these commonly inherited
344 cancer risk variants. We reasoned that p53 pathway genes with alleles which increase expression of
345 genes that inhibit p53 cell-killing activities and increase cancer risk, would be potential drug targets
346 to re-activate p53 through their inhibition.

347 In total, there are 1,133 GWAS implicated cancer-risk SNPs (lead SNPs and proxies) in 41 out
348 of 410 annotated p53 pathway genes (KEGG, BioCarta and PANTHER and/or direct p53 target
349 genes (33)) (**Fig. 3C**; **Supplementary Table S7**). To systematically identify those p53 pathway
350 genes with cancer risk SNPs whose increased expression associates with inhibition of p53-mediated
351 cancer cell killing, we looked to the above-described drug sensitivity dataset with both somatic
352 genetic and gene expression data (34). In total, the transcript levels of 3 of the 41 p53 pathway genes
353 that harbor cancer risk SNPs associate with Nutlin3 (the most significant compound associated with
354 *wtTP53* CNV status) sensitivities in cell lines with *wtTP53* and no copy number loss compared to
355 those with *TP53* mutations (KITLG, CDKN2A and TEX9; adjusted $p < 0.05$; **Fig. 3D**). For all three
356 of the significant associations, increased expression of these genes associates with increased

357 resistance to Nutlin3 treatment. In order to further validate these associations in terms of their
358 dependency on p53 activation and not solely Nutlin3 treatment, we explored similar associations in
359 the three noted DNA-damaging agents (Doxorubicin, Etoposide and Cisplatin) that demonstrated
360 sensitivities to *TP53* mutational status (**Fig. 3B**). Only for *KITLG* (**Fig. 3E**), did increased expression
361 levels associate with increased resistance towards all four agents.

362 **5. Increased expression of *KITLG* attenuates p53's anti-cancer activities**

363 There are multiple significant associations that are consistent with an inhibitory role of increased
364 *KITLG* expression on p53's anti-cancer activities in testicular germ cell tumors (TGCT), a cancer
365 type that rarely mutates *TP53*. First, relative to other cancer types, *KITLG* copy gain (GISTIC score
366 ≥ 1) is highly enriched in *wtTP53* TGCT (3.7-fold, adjusted $p = 2.9e-29$; **Fig. 4A**). Second, the TGCT
367 GWAS risk allele residing in *KITLG* is enriched in TGCT patients with *wtTP53* tumors relative to
368 the *wtTP53* tumors of other cancer types (**Fig. 4B**). Third, patients with elevated expression of
369 *KITLG* in *wtTP53* TGCT progress faster (**Fig. 4C**). Fourth, the TGCT GWAS risk locus falls within
370 an intron of *KITLG* occupied by p53 in many different cell types and under many different cellular
371 stresses (**Supplementary Fig. 2A**). This region contains 6 common SNPs that are in high linkage
372 disequilibrium (LD) in Europeans ($r^2 > 0.95$) (red square, **Fig. 4D**) (35,36), including a reported
373 polymorphic p53 response element (p53 RE SNP, rs4590952). The major alleles of this SNP
374 associate with increased TGCT risk, increased p53 binding, transcriptional enhancer activity, and
375 greater *KITLG* expression in heterozygous cancer cell lines wild type for *TP53* (37). Third, higher
376 grade, but not lower grade, *wtTP53* TGCT patients carrying alleles associated with increased risk
377 and *KITLG* expression also progress faster (**Fig. 4E and Supplementary Fig. 2B-C**;
378 **Supplementary Table S8**).

379 In order to experimentally test the potential inhibitory role of increased *KITLG* expression on
380 p53's anti-cancer activities in TGCT, we deleted the risk locus in two TGCT-derived cell lines
381 (TERA1 and TERA2) with *wtTP53* and homozygous for the TGCT risk alleles (p53-REs+/+) (**Fig.**
382 **4F and Supplementary Fig. S3A-C**). As predicted from the above-described associations, we found
383 significantly higher *KITLG* RNA levels in non-edited p53-REs+/+ clones, compared to either the
384 heterozygous knock outs (KOs) p53-REs+/- clones or the homozygous KOs REs-/- clones (**Fig. 4G**).
385 After Nutlin3 treatment, the p53-REs-/- clones showed no measurable induction of *KITLG* relative to
386 p53-RE+/+ cells (**Fig. 4H**, red bars versus grey bars). We found no significant differences between
387 the p53-REs-/- and p53-REs+/+ clones in other genes surrounding *KITLG* (± 1 Mbp; **Supplementary**
388 **Fig. S3D**). Re-integration of the deleted regions into its original locus rescued basal expression,
389 resulting in significantly higher *KITLG* RNA levels in the knock-in (KI) clones of both cell lines

390 relative to the p53-REs^{-/-} (**Fig. 4F and 4I; Supplementary Fig. S3E-G**). The KI clones also rescued
391 the p53-dependent induction of *KITLG* expression relative to the p53-REs^{-/-} (**Fig. 4I**).

392 *KITLG* is best known to act through the c-KIT receptor tyrosine kinase to promote cell survival
393 in many cancer types (38). To determine if heightened *KITLG*/c-KIT signaling inhibits p53's anti-
394 cancer activities in TGCT, we explored its impact on cellular sensitivities to p53-activating agents.
395 We found that deletion of the *KITLG* risk locus or c-KIT knock-down resulted in an increased
396 sensitivity to Nutlin3, and increased levels of cleaved caspase3 and PARP1 (**Fig. 5A-B;**
397 **Supplementary Fig. S4A-B**). We were able to rescue the increased Nutlin3 sensitivity and
398 caspase3/PARP1 cleavage of p53RE^{-/-} clones in KI cells (**Fig. 5A and Supplementary Fig.S4C**).
399 To further test the p53-dependence of these effects, we reduced *TP53* expression levels and observed
400 reduced expression of cleaved caspase3 after Nutlin3 treatment (**Supplementary Fig. S4D**), and an
401 overall insensitivity towards Nutlin3 in both p53-REs^{+/+} and p53-REs^{-/-} cells (**Supplementary Fig.**
402 **S4E**).

403 Thus-far, we have demonstrated that TGCT cells with increased expression of *KITLG* have
404 increased pro-cancer survival traits previously attributed to *KITLG*/cKIT signaling in other cancer
405 types. Moreover, these cells also have traits that suggest an inhibitory effect of *KITLG* on a p53-
406 associated anti-cancer activity, namely the apoptotic response to p53 activation after MDM2
407 inhibition with Nutlin3 treatment. To further explore this, we screened 317 anti-cancer compounds
408 to identify agents that, like Nutlin3, kill significantly more cells at lower concentrations in p53-RE^{-/-}
409 clones than in p53^{+/+} clones (**Fig. 5C**). We identified 198 compounds in the TERA1 screen and 112
410 compounds in the TERA2 screen that showed heightened sensitivity in p53-RE^{-/-} cells in at least one
411 of the 4 different concentrations tested (≥ 1.5 fold in both replicates; **Supplementary Fig. S5A**, blue
412 dots). One hundred of these agents overlapped between TERA1 and TERA2 (1.7-fold, $p = 1.1e-21$;
413 **Supplementary Fig. S5A**), suggesting a potential shared mechanism underling the differential
414 sensitivities. For example, two *MDM2* inhibitors in the panel of compounds, Nutlin3 and
415 Serdemetan, were among the 100 overlapping agents (**Fig. 5D; Supplementary Table S3**). We
416 found a significant and consistent enrichment of topoisomerase inhibitors in both cell lines among 14
417 different compound classes (14 compounds in TERA1 [100%] and 10 compounds in TERA2 [71%]
418 of 14 Topo inhibitors screened; **Fig. 5D-E**). To validate the genotype-specific effects of the
419 topoisomerase inhibitors, we determined the IC50 values of three of them (Doxorubicin,
420 Camptothecin, and Topotecan) using MTT measurements in multiple clones of TERA1 cells with
421 differing genotypes. All three agents showed a significant reduction of IC50 values, increased
422 sensitivities, in the p53-REs^{-/-} clones (lower *KITLG*) relative to the p53-REs^{+/+} clones (higher

423 *KITLG*) (**Supplementary Fig. S5B**). We were able to rescue this increased sensitivity to
424 topoisomerase inhibitors in the *p53RE*^{-/-} clones in KI cells (**Supplementary Fig. S5B**). Together,
425 these results demonstrate that TGCT cell lines with heightened *KITLG* expression mediated by the
426 risk locus, are less sensitive to 100 agents, most of which are known to activate p53-mediated cell
427 killing.

428 **6. Inhibition of *KITLG*/c-KIT signaling and p53 activation interact to kill treatment resistant** 429 **cancer cells**

430 There are many RTK inhibitors that are current therapeutic agents which inhibit c-KIT activity
431 (39). If p53-mediated *KITLG*-dependent pro-survival signaling can attenuate chemosensitivity to
432 p53-activating agents, RTK inhibitors should be able to interact synergistically with p53-activating
433 agents to kill TGCT cells. Indeed, co-modulation of these two pathways has shown promise in other
434 cancer types (40-42). We therefore tested which RTK inhibitor (known to inhibit c-KIT) kills TCGT
435 cells most efficiently. Of the five FDA-approved RTKs analyzed, Pazopanib, Imatinib, Nilotinib,
436 Sunitinib and Dasatinib, the most potent was Dasatinib (**Supplementary Fig. S5C**). To determine
437 potential synergy of RTKs with Nutlin3 in TGCT, we treated cells with Dasatinib, and quantitated
438 potential drug-drug interactions by calculating Combination Indices (CI). We observed clear
439 synergistic interactions (CI <1) between Nutlin3 and Dasatinib in both TERA1 and TERA2 *p53*-
440 *REs*^{+/+} cells (**Fig. 5F**, grey bars), and enhanced levels of cleaved caspase3 and PARP1, relative to
441 single drug treatments without altering p53 stabilization (**Supplementary Fig. S5D**). Consistent with
442 the requirement of the p53-dependent activation of *KITLG*, no synergy between Dasatinib and
443 Nutlin3 was detected in *p53-REs*^{-/-} cells (CI >1; **Fig. 5F**, red bars).

444 We next explored the interaction between Dasatinib and multiple DNA-damaging
445 chemotherapeutics known to activate p53. We focused on the 3 topoisomerase inhibitors
446 (Doxorubicin, Camptothecin and Topotecan), as well as Cisplatin, a chemotherapeutic agent used to
447 treat TGCT, and which induces DNA damage and p53. Dasatinib demonstrated significant levels of
448 synergy with each of the DNA-damaging agents tested in *p53-REs*^{+/+} cells (**Supplementary Fig.**
449 **S5E-F**). Similar to Nutlin3, no synergy was detected in *p53-REs*^{-/-} cells of either cell lines for any
450 combination of agents (**Supplementary Fig. S5E-F**). Furthermore, the synergistic interaction
451 between Dasatinib and the p53-activating agents Nutlin3 and Doxorubin could be rescued by
452 knocking in the p53-bound germline TGCT-risk locus in *KITLG* (**Fig. 5G**, orange bars).

453 Thus, a more effective therapeutic strategy for TGCT patients could be to modulate both the cell
454 death and cell survival functions of p53, through co-inhibition of p53/*KITLG*-mediated pro-survival

455 signaling together with the co-activation of p53-mediated anti-survival signaling. Such a therapeutic
456 combination could provide an alternative for patients with treatment-resistant disease (43). To
457 investigate this idea, we explored synergistic interactions between c-KIT inhibitor Dasatinib and p53
458 activators in cisplatin-resistant clones of GCT27 (GCT27-CR) and Susa (Susa-CR) (44), as well as in
459 the intrinsically cisplatin-resistant TGCT cell line 2102EP (45) with *wtTP53* and at least one copy of
460 the haplotype containing the KITLG risk allele SNPs. Similar to the observations in the cisplatin-
461 sensitive TGCT cell lines, Dasatinib and Doxorubicin interacted synergistically to kill all three
462 cisplatin-resistant clones and cell lines (**Fig. 5H**). Moreover, co-treatment with Dasatinib and
463 Doxorubicin of Susa-CR and 2102EP led to a significant reduction (~20-fold, on average) in the
464 concentrations of Dasatinib and Doxorubicin used to achieve IC₅₀ relative to when the drugs are
465 used individually (**Supplementary Fig. S5G**). To determine if the combination treatment could
466 show a greater efficacy in treating tumors, we generated a subcutaneous xenograft model using the
467 2102EP cell line, and treated the mice with two approved drugs Dasatinib and Doxorubicin either
468 alone or in combination. Consistent with the observations made in cell culture, treatment of mice
469 engrafted with 2102EP cells revealed stronger anti-tumoral effects with the Dasatinib/Doxorubicin
470 pair relative to single drug treatments (**Fig. 5I**). This dosing regimen was well tolerated with no body
471 weight loss in mice (**Supplementary Fig. S5H**).

472 **7. KITLG/c-KIT signaling interacts with p53 to affect cancer progression and drug response in** 473 **melanoma**

474 Our results clearly support a model, whereby increased expression of *KITLG* mediated by the
475 region with the TGCT cancer risk SNP(s) heightens KITLG/c-KIT signaling and attenuates p53
476 activity, thereby allowing for the retention and re-activation of *wtTP53* in testicular cancer cells. The
477 *KITLG* testicular cancer risk SNP(s) have yet to be found to associate with other cancer types (46),
478 suggesting a tissue-specificity of this locus with transcriptional enhancer activity. However, other
479 genetic variants that elevate KITLG/c-KIT signaling could also attenuate p53 activity, and thus allow
480 for the retention and ultimate re-activation of *wtTP53* in cancer cells. To test this, we focused on
481 known somatic driver mutations of *c-KIT* in the TCGA cohort. If our model is correct, we would
482 expect the majority of tumors with activating *c-KIT* mutations to retain a *wtTP53* locus. Indeed, 43
483 out of 6,997 (0.61%) patients with *wtTP53* tumors also have oncogenic *c-KIT* mutations relative to
484 just 10 out of 3,735 (0.27%) of *TP53* mutant tumors (**Fig. 6A**; OR = 2.3, p = 0.014).

485 As expected, the tumor types enriched in c-KIT oncogenic mutations in the TCGA cohort are
486 cancers known to be driven by KIT signaling (38). Testicular cancers (TGCT; 13.6%; 20 out of
487 147), skin cutaneous melanoma (SKCM; 3.9%; 14 out of 356) and acute myeloid leukemias (AML;

488 2.8%; 5 out of 181) have proportionally more *c-KIT* mutations than all *wtTP53* tumors (0.61%)
489 (adjusted $p < 0.05$; **Fig. 6B** left panel). It is important to note that these enrichments are only
490 significant when *wtTP53* without *TP53*-loss, but not *TP53* loss or mutant tumors are considered (**Fig.**
491 **6B**). If our model is correct and inhibition of c-KIT signaling will re-activate p53's ability to kill the
492 *wtTP53* cancers, we would expect, like in TGCT, that elevated *KITLG* levels will associate with
493 faster progression and/or poorer survival of the cancers with both wild-type *TP53* and *c-KIT*.
494 Indeed, in both melanoma and AML, we observed the association between heightened *KITLG*
495 expression and poorer clinical outcomes (**Fig. 6C**, the TCGA-SKCM cohort; **Fig. 6D** the TCGA-
496 AML cohort). Consistent associations were observed in an independent cohort (DFCI-SKCM) of 35
497 *wtTP53* melanoma patients (**Fig. 6E**), for which both the somatic genetic and expression data are
498 available (47). Importantly, we found that in melanoma and AML patients with *wtTP53* and no copy
499 number loss tumors, those with heightened *KITLG* expression have significantly poorer outcomes,
500 but not in patients with *TP53* mutant or copy number loss (**Fig. 6F-G**). Together these observations,
501 suggest that heightened *KITLG/cKIT* signaling in AML and melanoma could attenuate p53 activity
502 allowing for wt *TP53* retention and re-activation using cKIT inhibitors. In further support of this, in
503 AML, it has been shown that the c-Kit inhibitor Dasatinib does enhance p53-mediated cell killing
504 (40). Similarly, when we treated melanoma cells (SKMEL5 with wild type *TP53* and *c-KIT*) with
505 Dasatinib and the p53 activating agents Nutlin3 or Doxorubicin, we observed clear synergistic
506 interactions (**Fig. 6H**, CI <1; $p = 0.0013$ between Nutlin3 and Dasatinib and $p = 0.00066$ between
507 Doxorubicin and Dasatinib).

508

509 Discussion

510 In this study, we demonstrate that germline cancer-risk SNPs could influence cancer progression
511 and potentially provide information guiding precision medicine therapy decisions. Our work
512 highlights that even small relative reductions in *wtTP53* expression, mediated either by the minor
513 allele of the p53 poly(A) SNP or through loss of at least one copy of *TP53*, can reduce relative p53
514 cellular activity in cancer cells and overall survival of patients. Patients with either of these genetic
515 variations represent a large proportion of cancer patients. Patients with the minor allele of the SNP
516 and *wtTP53* in their cancers are found in 2.6% of the total TCGA cohort, with up to 5.9% in certain
517 cancer types. Overall, in the TCGA, 26.6% of patients have cancers wherein at least one copy of
518 *wtTP53* is lost with up to 73.1% in certain cancer types. In terms of including *TP53* status in
519 prognosis for patients, *TP53* mutation is often what is looked at most. Our work suggests that
520 *wtTP53* copy number loss could also add additional information to those patients that retain *wtTP53*.

521 Indeed, patients with tumors that express lower *wtTP53* levels will be interesting to study more in
522 depth to understand how to increase *wtTP53* levels to improve treatments, such as increasing
523 transcription of *wtTP53*, inhibiting miRNAs or blocking alternative polyadenylation.

524 The p53 stress response pathway inhibits cell survival, mediating both tumor suppression and
525 cellular responses to many cancer therapeutics (48). p53 also targets pro-survival genes. Activation
526 of these genes in tumors retaining *wtTP53* provide a survival advantage (49). We provide human
527 genetic evidence that also supports a tumor-promoting role of p53 pro-survival activities and, in the
528 case of the TGCT risk locus, points to the development of more effective therapy combinations
529 through the inhibition of these pro-survival activities in tumors that retain p53 activity. Although
530 TGCTs are one of the most curable solid tumors, men diagnosed with metastatic TGCT develop
531 platinum resistant disease and die at an average age of 32 years (43). There have been few new
532 treatments developed in the last two decades, and current therapeutic approaches can, importantly in
533 context of a cancer of young men, result in significant survivorship issues, including sustained
534 morbidities and delayed major sequelae (43). Our observations suggest the TGCT *KITLG* risk allele
535 in the polymorphic p53 enhancer leads to increased p53-dependent activation of the pro-survival
536 target gene, *KITLG*, which increases TGCT survival rather than senescence/apoptosis in the presence
537 of active p53. We demonstrate that co-inhibition of c-KIT and p53 activation interact synergistically
538 to kill platinum-resistant TGCTs with a drug combination (Dasatinib and Doxorubicin) that had
539 limited toxicity in a Phase II clinical trial (50), suggesting that an effective therapeutic strategy for
540 treatment-resistant TGCTs could be to modulate both the cell-death and cell-survival functions of
541 *wtTP53* cancers.

542 Using the most well-studied somatic mutation known to enhance *KITLG/c-KIT* signalling (*c-*
543 *KIT* mutations), we were able to identify SKCM as another potential repurposing opportunity for
544 combination therapies which inhibit *KITLG/c-KIT* signalling and activate p53. The role of c-KIT
545 signalling in the skin is well established with the pathway of crucial importance for the development
546 of melanocytes (51). In line with previous work, we found *wtTP53* SKCM to be enriched for c-KIT
547 mutations (52,53). Furthermore, we found high *KITLG* expression to associate independently with
548 poorer overall survival in *wtTP53* SKCM patients. Our data provides molecular support for targeting
549 of *KITLG/c-KIT* in melanoma. Melanoma rarely mutates *TP53* and expresses high levels of p53
550 protein, in line with the fact that SKCM is enriched for *wtTP53* and no *TP53* copy number loss (54).
551 Melanomas are hardwired to be resistant to p53 dependent apoptosis, perhaps because melanocytes
552 are programmed to survive UV light (55). Several mechanisms have been proposed for this
553 inhibition of p53 triggered apoptosis, including the action of iASPP, deletion of the *CDKN2A* locus,

554 aberrant phosphorylation of p53 and activation of MDM2 by downstream c-KIT signalling (55,56).
555 More recently, it has been shown that WNT5a signalling and wild-type p53 might co-operate in
556 melanoma to drive cells into a slow cycling state which is therapy resistant (57). It is possible that
557 KITLG/c-KIT-mediated inhibition of the p53-apoptotic response adds a further mechanism through
558 which *wtTP53* can be inhibited in melanoma without mutation, and opens up the possibility of
559 harnessing the pro-apoptotic function of p53 by inhibiting the KITLG/c-KIT pathway. Indeed, we
560 showed that the combination of Dasatinib and Nutlin-3a and Dasatinib and Doxorubicin are
561 synergistic in a wild-type *TP53* and *c-KIT* SKCM cell-line.

562 Unlike other tumor suppressors, complete loss of p53 activity is not a requirement for cancer
563 initiation. Reduction of p53 activity below a critical threshold through mutations is apparently
564 necessary and sufficient for cancer development (58). These mutations are primarily missense
565 mutations that affect p53's ability to bind to DNA in a sequence-specific manner and regulate
566 transcription of its target genes. These same mutations when found constitutionally result in Li-
567 Fraumeni Syndrome: a syndrome comprising dramatic increase in cancer risk in many tissues types.
568 These missense mutations may benefit cancers not simply through loss of p53 function, but also
569 through dominant-negative and gain-of-function activities (59). In mice, knock-in *TP53* gain-of-
570 function mutants displayed a more diverse set of, and more highly metastatic tumors than *TP53*
571 knock-out mutants (60,61). Many of the factors that regulate wild-type p53 tumor suppression can
572 also regulate mutant p53, including its pro-cancer activities. For example, wild-type p53 mice that
573 express lower levels of MDM2 show increased p53 levels, a better p53 stress response, and greater
574 tumor suppression, resulting in later and reduced tumor onset in many tissue types. Mutant p53
575 levels are also increased in these murine models, but cancers are found to arise earlier and harbor
576 gain-of-function metastatic phenotypes (62).

577 We go on to discuss that our SNP association with inverted cancer risk and somatic *TP53*
578 mutational status in humans reveal a similar scenario. Specifically, we demonstrated that the C-allele
579 of the p53 poly(A) SNP which can lead to decreased wild type and mutant p53 levels in tumors,
580 associates with an increased risk of *wtTP53* cancers, but decreased risk of sub-types with primarily
581 mutant *TP53*. For example, women with the minor allele associated with an increased risk for the
582 more *TP53* wild-type breast and ovarian subtypes and a decreased risk for the more mutant subtypes.
583 We also demonstrated that the TCGA pan-cancer or breast patients with *wtTP53* tumors and carrying
584 the C allele have shorter PFI compared to patients with *wtTP53* tumors without the C allele. Of note,
585 an inverted trend was found for mutant *TP53* tumors. Together, these observations support a role for
586 germline p53 pathway SNPs not only in modulating risk of disease and tumor biology in *wtTP53*

587 cancers but also in *TP53* mutant cancers, wherein alleles that increase mutant p53 levels would also
588 increase its pro-cancer activities.

589

590 **Acknowledgments**

591 This work was funded in part by the Ludwig Institute for Cancer Research, the Nuffield Department
592 of Medicine, the Development Fund, Oxford Cancer Research Centre, University of Oxford, UK, by
593 the Intramural Research Program of the National Institute of Environmental Health Sciences-
594 National Institutes of Health (Z01-ES100475), and NIH grant (DP5-OD017937), US, and by the S-
595 CORT Consortium from the Medical Research Council and Cancer Research UK.

596

597 **References**

- 598 1. Dancey JE, Bedard PL, Onetto N, Hudson TJ. The genetic basis for cancer treatment
599 decisions. *Cell* **2012**;148(3):409-20
- 600 2. Huang M, Shen A, Ding J, Geng M. Molecularly targeted cancer therapy: some lessons from
601 the past decade. *Trends Pharmacol Sci* **2014**;35(1):41-50
- 602 3. Carter H, Marty R, Hofree M, Gross AM, Jensen J, Fisch KM, *et al.* Interaction Landscape of
603 Inherited Polymorphisms with Somatic Events in Cancer. *Cancer discovery* **2017**;7(4):410-23
- 604 4. Lu C, Xie M, Wendl MC, Wang J, McLellan MD, Leiserson MD, *et al.* Patterns and
605 functional implications of rare germline variants across 12 cancer types. *Nature*
606 *communications* **2015**;6:10086
- 607 5. Yurgelun MB, Chenevix-Trench G, Lippman SM. Translating Germline Cancer Risk into
608 Precision Prevention. *Cell* **2017**;168(4):566-70
- 609 6. Stracquadanio G, Wang XT, Wallace MD, Grawenda AM, Zhang P, Hewitt J, *et al.* The
610 importance of p53 pathway genetics in inherited and somatic cancer genomes. *Nature*
611 *Reviews Cancer* **2016**;16(4):251-65
- 612 7. Martincorena I, Raine KM, Gerstung M, Dawson KJ, Haase K, Van Loo P, *et al.* Universal
613 Patterns of Selection in Cancer and Somatic Tissues. *Cell* **2017**;171(5):1029-41 e21
- 614 8. Kasthuber ER, Lowe SW. Putting p53 in Context. *Cell* **2017**;170(6):1062-78
- 615 9. Bouwman P, Jonkers J. The effects of deregulated DNA damage signalling on cancer
616 chemotherapy response and resistance. *Nature reviews Cancer* **2012**;12(9):587-98
- 617 10. Lowe SW, Ruley HE, Jacks T, Housman DE. P53-Dependent Apoptosis Modulates the
618 Cytotoxicity of Anticancer Agents. *Cell* **1993**;74(6):957-67
- 619 11. Weinstein JN, Myers TG, O'Connor PM, Friend SH, Fornace AJ, Jr., Kohn KW, *et al.* An
620 information-intensive approach to the molecular pharmacology of cancer. *Science*
621 **1997**;275(5298):343-9
- 622 12. Willer CJ, Li Y, Abecasis GR. METAL: fast and efficient meta-analysis of genomewide
623 association scans. *Bioinformatics* **2010**;26(17):2190-1
- 624 13. Liu JF, Lichtenberg T, Hoadley KA, Poisson LM, Lazar AJ, Cherniack AD, *et al.* An
625 Integrated TCGA Pan-Cancer Clinical Data Resource to Drive High-Quality Survival
626 Outcome Analytics. *Cell* **2018**;173(2):400-+
- 627 14. Ran FA, Hsu PD, Wright J, Agarwala V, Scott DA, Zhang F. Genome engineering using the
628 CRISPR-Cas9 system. *Nature protocols* **2013**;8(11):2281-308

- 629 15. Zhang P, Elabd S, Hammer S, Solozobova V, Yan H, Bartel F, *et al.* TRIM25 has a dual
630 function in the p53/Mdm2 circuit. *Oncogene* **2015**;34(46):5729-38
- 631 16. Chou TC. Theoretical basis, experimental design, and computerized simulation of synergism
632 and antagonism in drug combination studies. *Pharmacol Rev* **2006**;58(3):621-81
- 633 17. Stacey SN, Sulem P, Jonasdottir A, Masson G, Gudmundsson J, Gudbjartsson DF, *et al.* A
634 germline variant in the TP53 polyadenylation signal confers cancer susceptibility. *Nature*
635 *genetics* **2011**;43(11):1098-103
- 636 18. Consortium GT. The Genotype-Tissue Expression (GTEx) project. *Nature genetics*
637 **2013**;45(6):580-5
- 638 19. Deng Q, Hu H, Yu X, Liu S, Wang L, Chen W, *et al.* Tissue-specific microRNA expression
639 alters cancer susceptibility conferred by a TP53 noncoding variant. *Nature communications*
640 **2019**;10(1):5061
- 641 20. Rafnar T, Gunnarsson B, Stefansson OA, Sulem P, Ingason A, Frigge ML, *et al.* Variants
642 associating with uterine leiomyoma highlight genetic background shared by various cancers
643 and hormone-related traits. *Nature communications* **2018**;9(1):3636
- 644 21. Zhang H, Ahearn TU, Lecarpentier J, Barnes D, Beesley J, Qi G, *et al.* Genome-wide
645 association study identifies 32 novel breast cancer susceptibility loci from overall and
646 subtype-specific analyses. *Nature genetics* **2020**;52(6):572-81
- 647 22. Landi MT, Bishop DT, MacGregor S, Machiela MJ, Stratigos AJ, Ghiorzo P, *et al.* Genome-
648 wide association meta-analyses combining multiple risk phenotypes provide insights into the
649 genetic architecture of cutaneous melanoma susceptibility. *Nature genetics* **2020**;52(5):494-
650 504
- 651 23. Rashkin SR, Graff RE, Kachuri L, Thai KK, Alexeeff SE, Blatchins MA, *et al.* Pan-cancer
652 study detects genetic risk variants and shared genetic basis in two large cohorts. *Nature*
653 *communications* **2020**;11(1):4423
- 654 24. Cancer Genome Atlas N. Comprehensive molecular portraits of human breast tumours.
655 *Nature* **2012**;490(7418):61-70
- 656 25. Cancer Genome Atlas Research N. Integrated genomic analyses of ovarian carcinoma. *Nature*
657 **2011**;474(7353):609-15
- 658 26. Michailidou K, Lindstrom S, Dennis J, Beesley J, Hui S, Kar S, *et al.* Association analysis
659 identifies 65 new breast cancer risk loci. *Nature* **2017**;551(7678):92-4
- 660 27. Phelan CM, Kuchenbaecker KB, Tyrer JP, Kar SP, Lawrenson K, Winham SJ, *et al.*
661 Identification of 12 new susceptibility loci for different histotypes of epithelial ovarian
662 cancer. *Nature genetics* **2017**;49(5):680-91
- 663 28. Suh YA, Post SM, Elizondo-Fraire AC, Maccio DR, Jackson JG, El-Naggar AK, *et al.*
664 Multiple stress signals activate mutant p53 in vivo. *Cancer Res* **2011**;71(23):7168-75
- 665 29. Yue X, Zhao Y, Xu Y, Zheng M, Feng Z, Hu W. Mutant p53 in Cancer: Accumulation, Gain-
666 of-Function, and Therapy. *J Mol Biol* **2017**;429(11):1595-606
- 667 30. Burckstummer T, Banning C, Hainzl P, Schobesberger R, Kerzendorfer C, Pauler FM, *et al.*
668 A reversible gene trap collection empowers haploid genetics in human cells. *Nature methods*
669 **2013**;10(10):965-71
- 670 31. Gudkov AV, Komarova EA. The role of p53 in determining sensitivity to radiotherapy.
671 *Nature reviews Cancer* **2003**;3(2):117-29
- 672 32. Hientz K, Mohr A, Bhakta-Guha D, Efferth T. The role of p53 in cancer drug resistance and
673 targeted chemotherapy. *Oncotarget* **2017**;8(5):8921-46
- 674 33. Fischer M. Census and evaluation of p53 target genes. *Oncogene* **2017**;36(28):3943-56
- 675 34. Iorio F, Knijnenburg TA, Vis DJ, Bignell GR, Menden MP, Schubert M, *et al.* A Landscape
676 of Pharmacogenomic Interactions in Cancer. *Cell* **2016**;166(3):740-54

- 677 35. Turnbull C, Rapley EA, Seal S, Pernet D, Renwick A, Hughes D, *et al.* Variants near
678 DMRT1, TERT and ATF7IP are associated with testicular germ cell cancer. *Nature genetics*
679 **2010**;42(7):604-U178
- 680 36. Litchfield K, Levy M, Orlando G, Loveday C, Law PJ, Migliorini G, *et al.* Identification of
681 19 new risk loci and potential regulatory mechanisms influencing susceptibility to testicular
682 germ cell tumor. *Nature genetics* **2017**;49(7):1133-+
- 683 37. Zeron-Medina J, Wang X, Repapi E, Campbell MR, Su D, Castro-Giner F, *et al.* A
684 polymorphic p53 response element in KIT ligand influences cancer risk and has undergone
685 natural selection. *Cell* **2013**;155(2):410-22
- 686 38. Lennartsson J, Ronnstrand L. Stem cell factor receptor/c-Kit: from basic science to clinical
687 implications. *Physiological reviews* **2012**;92(4):1619-49
- 688 39. Flaherty KT, Hodi FS, Fisher DE. From genes to drugs: targeted strategies for melanoma.
689 *Nature reviews Cancer* **2012**;12(5):349-61
- 690 40. Dos Santos C, McDonald T, Ho YW, Liu H, Lin A, Forman SJ, *et al.* The Src and c-Kit
691 kinase inhibitor dasatinib enhances p53-mediated targeting of human acute myeloid leukemia
692 stem cells by chemotherapeutic agents. *Blood* **2013**;122(11):1900-13
- 693 41. Henze J, Muhlenberg T, Simon S, Grabellus F, Rubin B, Taeger G, *et al.* p53 Modulation as
694 a Therapeutic Strategy in Gastrointestinal Stromal Tumors. *Plos One* **2012**;7(5)
- 695 42. Kurosu T, Wu N, Oshikawa G, Kagechika H, Miura O. Enhancement of imatinib-induced
696 apoptosis of BCR/ABL-expressing cells by nutlin-3 through synergistic activation of the
697 mitochondrial apoptotic pathway. *Apoptosis : an international journal on programmed cell*
698 *death* **2010**;15(5):608-20
- 699 43. Litchfield K, Levy M, Huddart RA, Shipley J, Turnbull C. The genomic landscape of
700 testicular germ cell tumours: from susceptibility to treatment. *Nat Rev Urol* **2016**;13(7):409-
701 19
- 702 44. Noel EE, Yeste-Velasco M, Mao X, Perry J, Kudahetti SC, Li NF, *et al.* The association of
703 CCND1 overexpression and cisplatin resistance in testicular germ cell tumors and other
704 cancers. *The American journal of pathology* **2010**;176(6):2607-15
- 705 45. Koster R, di Pietro A, Timmer-Bosscha H, Gibcus JH, van den Berg A, Suurmeijer AJ, *et al.*
706 Cytoplasmic p21 expression levels determine cisplatin resistance in human testicular cancer.
707 *The Journal of clinical investigation* **2010**;120(10):3594-605
- 708 46. Buniello A, MacArthur JAL, Cerezo M, Harris LW, Hayhurst J, Malangone C, *et al.* The
709 NHGRI-EBI GWAS Catalog of published genome-wide association studies, targeted arrays
710 and summary statistics 2019. *Nucleic acids research* **2019**;47(D1):D1005-D12
- 711 47. Van Allen EM, Miao D, Schilling B, Shukla SA, Blank C, Zimmer L, *et al.* Genomic
712 correlates of response to CTLA-4 blockade in metastatic melanoma. *Science*
713 **2015**;350(6257):207-11
- 714 48. Vazquez A, Bond EE, Levine AJ, Bond GL. The genetics of the p53 pathway, apoptosis and
715 cancer therapy. *Nat Rev Drug Discov* **2008**;7(12):979-87
- 716 49. Kruiswijk F, Labuschagne CF, Vousden KH. p53 in survival, death and metabolic health: a
717 lifeguard with a licence to kill. *Nat Rev Mol Cell Bio* **2015**;16(7):393-405
- 718 50. Benjamini O, Dumlaio TL, Kantarjian H, O'Brien S, Garcia-Manero G, Faderl S, *et al.* Phase
719 II trial of HyperCVAD and Dasatinib in patients with relapsed Philadelphia chromosome
720 positive acute lymphoblastic leukemia or blast phase chronic myeloid leukemia. *American*
721 *journal of hematology* **2014**;89(3):282-7
- 722 51. Wehrle-Haller B. The role of Kit-ligand in melanocyte development and epidermal
723 homeostasis. *Pigment cell research / sponsored by the European Society for Pigment Cell*
724 *Research and the International Pigment Cell Society* **2003**;16(3):287-96
- 725 52. Beadling C, Jacobson-Dunlop E, Hodi FS, Le C, Warrick A, Patterson J, *et al.* KIT gene
726 mutations and copy number in melanoma subtypes. *Clin Cancer Res* **2008**;14(21):6821-8

- 727 53. Curtin JA, Busam K, Pinkel D, Bastian BC. Somatic activation of KIT in distinct subtypes of
728 melanoma. *J Clin Oncol* **2006**;24(26):4340-6
- 729 54. McGregor JM, Yu CC, Dublin EA, Barnes DM, Levison DA, MacDonald DM. p53
730 immunoreactivity in human malignant melanoma and dysplastic naevi. *The British journal of*
731 *dermatology* **1993**;128(6):606-11
- 732 55. Box NF, Vukmer TO, Terzian T. Targeting p53 in melanoma. *Pigment cell & melanoma*
733 *research* **2014**;27(1):8-10
- 734 56. Lu M, Breysens H, Salter V, Zhong S, Hu Y, Baer C, *et al.* Restoring p53 function in human
735 melanoma cells by inhibiting MDM2 and cyclin B1/CDK1-phosphorylated nuclear iASPP.
736 *Cancer cell* **2013**;23(5):618-33
- 737 57. Webster MR, Fane ME, Alicea GM, Basu S, Kossenkov AV, Marino GE, *et al.* Paradoxical
738 Role for Wild-Type p53 in Driving Therapy Resistance in Melanoma. *Molecular cell*
739 **2020**;77(3):681
- 740 58. Hohenstein P. Tumour suppressor genes--one hit can be enough. *PLoS biology*
741 **2004**;2(2):E40
- 742 59. Muller PA, Vousden KH. Mutant p53 in cancer: new functions and therapeutic opportunities.
743 *Cancer cell* **2014**;25(3):304-17
- 744 60. Lang GA, Iwakuma T, Suh YA, Liu G, Rao VA, Parant JM, *et al.* Gain of function of a p53
745 hot spot mutation in a mouse model of Li-Fraumeni syndrome. *Cell* **2004**;119(6):861-72
- 746 61. Olive KP, Tuveson DA, Ruhe ZC, Yin B, Willis NA, Bronson RT, *et al.* Mutant p53 gain of
747 function in two mouse models of Li-Fraumeni syndrome. *Cell* **2004**;119(6):847-60
- 748 62. Terzian T, Suh YA, Iwakuma T, Post SM, Neumann M, Lang GA, *et al.* The inherent
749 instability of mutant p53 is alleviated by Mdm2 or p16INK4a loss. *Genes & development*
750 **2008**;22(10):1337-44

751

752 **Figure Legends**

753 **Figure 1. A p53 regulatory cancer risk SNP associates with subtype heterogeneity risk.** (A) Pie
754 charts of the percentages of oncogenic and loss-of-function p53 mutations found amongst all known
755 pathogenic p53 missense mutations in breast and ovarian cancers. (B) A proposed model of how the
756 p53 poly(A) SNP could modify the ability of mutant p53 to drive cancer and of wild type p53 to
757 suppress it. (C) Forest plots illustrating the associations of the p53 poly(A) SNP with breast cancer
758 and ovarian cancer subtypes. The odd ratios (OR) are plotted for the SNP and subtype, and the error
759 bars represent the associated 95% confidence intervals (CI). (D) A schematic overview of the
760 association testing between the SNP and p53 mutational status in TCGA tumors. (E) A bar plot of
761 the minor allele frequencies (MAFs) of the p53 poly(A) SNP in patients with either *wtTP53* tumors
762 or mutant *TP53* tumors.

763

764 **Figure 2. A p53 regulatory cancer risk SNP and somatic copy number loss of p53 associates**
765 **with clinical outcomes.** (A) A box plot of *TP53* mRNA expression levels in 3,248 tumors from
766 individuals with differing genotypes of the p53 poly(A) SNP. The fold change of median *TP53*
767 expression between genotypes, the p-value (linear regression) and beta coefficients of the association
768 of the genotype with mRNA levels are depicted. (B) A schematic diagram of the *TP53* mutational
769 status and CRISPR-editing strategy in Hap1 cells. (C) A bar plot of *TP53* mRNA levels for each
770 genotype in Hap1 cells, measured using qRT-PCR normalized to GAPDH. Error bars represent SEM
771 of 3 independent experiments. p-values were calculated using a two-tailed t-test. (D) A forest plot of
772 the PFI and OS of cancer patients (pan-cancer TCGA cohort) stratified by the somatic *TP53*
773 mutational status. Hazard ratios (HR) and p values were calculated using Cox proportional hazards
774 model. (E) Kaplan-Meier survival curves for PFI in a total of 381 breast cancer patients carrying
775 either the major or the minor allele of the p53 poly(A) SNP and/or somatic *TP53* mutations. Curves
776 were truncated at 10 years, but the statistical analyses were performed using all of the data (logrank
777 test). (F) A bar plot showing the percentage of non-responders in each group stratified by the somatic
778 or germline *TP53* alterations as indicated on the x axis. Numbers of patients (number of non-
779 responders / total number of patients) in each group are indicated within the bars. p values were
780 calculated by two-tailed Fisher's exact test (*p<0.05, **p<0.005). (G) Box plots of *TP53* mRNA
781 expression levels in *wtTP53* tumors (left panel) and mutant *TP53* tumors (right panel) from
782 individuals with differing *TP53* copy number status. (H) A forest plot of PFI and OS of TCGA
783 cancer patients stratified by the somatic *TP53* mutational status. HR comparing PFI and OS in
784 patients with or without *TP53* copy number loss are indicated on the right. (I) A bar plot showing the

785 percentage of non-responders in each group stratified by the *TP53* mutations and copy number loss
786 as indicated on the x axis.

787

788 **Figure 3. Copy number loss of *TP53* and increased expression of a druggable pathway gene**
789 **with cancer risk SNPs dampens p53's anti-cancer activities.** (A) Box plots of p53 mRNA
790 expression levels in *wtTP53* cells (left panel) and mutant *TP53* cells (right panel) with differing
791 *TP53* copy number statuses. (B) Volcano plots of 304 drugs and their association with differential
792 sensitivities in cancer cell lines with *TP53* copy number loss relative to cell lines without *TP53* copy
793 number loss (left: *wtTP53* cells; right: mutant *TP53* cells). $-\text{Log}_{10}$ adjusted p-values (linear
794 regression and FDR-adjusted) are plotted against the beta coefficient. The horizontal dashed lines
795 represent the FDR-adjusted p value of 0.05. (C) A Chord Diagram of 102 cancer GWAS lead SNPs
796 in 41 p53 pathway genes that associate with differential risk to a total of 19 different cancer types.
797 The width of the connecting bands indicate the number of lead SNPs for each association. A dot plot
798 of the odds ratios for each association is presented in the inner circle and with red dots. The median
799 odd ratio for each association is presented in parentheses next to the gene name. (D) Volcano plots of
800 the associations between the transcript levels of the 41 p53 pathway cancer GWAS genes and
801 Nutlin3 sensitivities in cancer cell lines with either *wtTP53*-no.loss (upper panel) or *TP53* mutant-
802 loss (lower panel). (E) Box plots of the Log_2 IC50 values of p53 activating agents in cells either with
803 low, intermediate or high *KITLG* mRNA levels and *wtTP53*-no.loss.

804

805 **Figure 4. The p53-bound cancer risk locus in *KITLG* associates with patient outcome and**
806 **attenuates p53's anti-cancer activities.** (A-B) Dot plots showing the enrichment of *KITLG* copy
807 number gains (A) and risk allele frequencies (B) across TCGA cancer types. $-\text{Log}_{10}$ adjusted p-
808 values are plotted against the Log_2 fold change of the percentage of tumors with *KITLG* gains/risk
809 alleles in a given cancer type vs. the other cancers combined. (C) A Kaplan-Meier survival curve for
810 PFI in p53wt testicular cancer patients with high or low *KITLG* mRNA expression. p value was
811 calculated using log-rank test. (D) Genetic fine mapping identified 6 SNPs with the strongest TGCT
812 GWAS signal and which are in high linkage disequilibrium (r^2) in Europeans (red square). (E) A
813 Kaplan-Meier survival curve for PFI in high-stage p53wt testicular cancer patients carrying either the
814 risk (orange) or the non-risk allele (grey) of the *KITLG* risk SNP. (F) A diagram of the CRISPR-
815 editing utilized. (G) *KITLG* gene expression in CRISPR-edited clones using qRT-PCR normalized to
816 GAPDH. In total, 2 to 3 clones of each genotype were analyzed in 3 independent biological
817 replicates. p-values were calculated using a one-way ANOVA, followed by Tukey's multiple

818 comparison test. (H) A bar graph of the fold change in *KITLG* expression after Nutlin3 treatment,
819 Error bars represent SEM of 2 clones for each genotype and in 2 independent experiments. p-values
820 were calculated using a two-tailed t-test. (I) Dot plots of *KITLG* expression in CRISPR-edited
821 clones.

822

823 **Figure 5. p53/KITLG pro-survival signaling can attenuate responses to p53-activating agents.**

824 (A) Bar blots of the IC50 values for Nutlin3. p-values were calculated using a two-tailed t-test and
825 error bars represent SEM in at least 3 independent biological replicates. (B) Western blot analysis of
826 cells that were treated with or without Nutlin3 for 6 hours, lysed and analyzed for p53, acetylated
827 p53, Parp1 and cleaved-caspase3 protein expression. (C) Schematic overview for the microscopy-
828 based high-content drug screening. (D) Bar plots depicting the number of hits and “non-hits” for
829 each of the 14 drug classes examined. (E) Scatter plots of the fold enrichment of hits amongst each
830 drug class relative to the total compounds in the 14 drug classes. The horizontal dashed lines
831 represent the FDR-adjusted p value of 0.05. (F-G) Bar plots of combination indexes of Dasatinib
832 with Nutlin3 (F) or Doxorubicin (G) in p53-REs+/+ (grey bars, two clones), p53-REs-/- (red bars,
833 two clones) and knock-in clones (orange bars, one clone) of TERA1 and TERA2 cells. (H) Bar plots
834 of combination indexes of Dasatinib with Nutlin3 or Doxorubicin in panel of TGCT cell lines. (I)
835 Growth curves of 2102EP xenograft tumors treated with vehicle, Doxorubicin, Dasatinib or the
836 combination of Doxorubicin and Dasatinib. Error bars represent means \pm SEM (n=6).

837

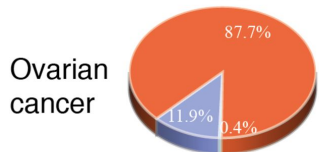
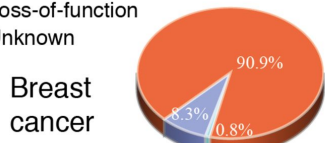
838 **Figure 6. KITLG/c-KIT signaling interacts with p53 to affect cancer progression and drug**

839 **response in melanoma.** (A) A bar graph of the percentage of oncogenic *c-KIT* mutations in *wtTP53*
840 tumors relative to *TP53* mutant tumors. (B) Scatter plots of the fold enrichment of oncogenic *c-KIT*
841 mutations in a given cancer type relative to all cKIT mutation in pan-cancer. The horizontal dashed
842 lines represent the FDR-adjusted p value of 0.05. (C-E) Kaplan-Meier survival curves for OS (C, left
843 panel) and PFI (C, right panel) in TCGA-SKCM patients, for OS (D) in TCGA-AML patients, and
844 for OS (E, left panel) and DFS (E, right panel) in DFCI-SKCM patients stratified based on *KITLG*
845 mRNA levels. (F-G) Two forest plots of PFI and OS of TCGA cancer patients (F: SKCM; G: AML)
846 stratified by the somatic *TP53* mutational status. HR and p values were calculated using Cox
847 proportional hazards model. (H) A bar plot of combination indexes of Dasatinib with Nutlin3 or
848 Doxorubicin in melanoma cells. p values were calculated by one-sample t-test. Error bars represent
849 means \pm SEM (n=3).

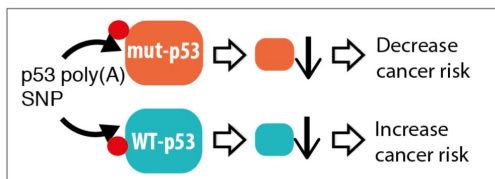
Figure 1

A *TP53* pathogenic missense mutation

- Oncogenic
- Loss-of-function
- Unknown

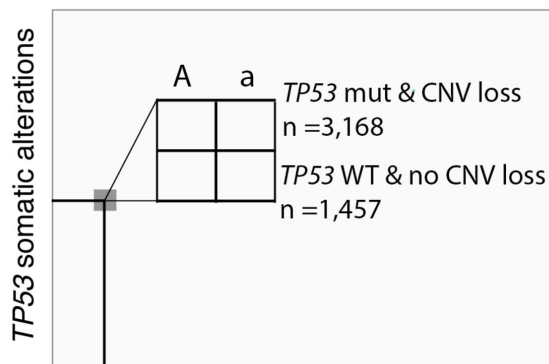


B



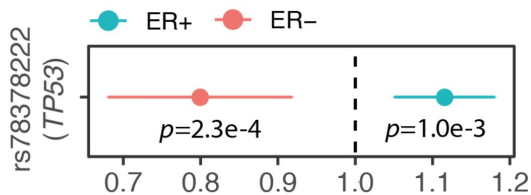
D

TCGA Case-only association testing

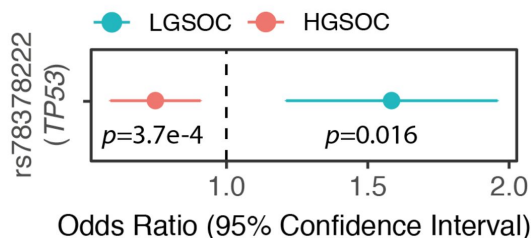


C

Breast cancer



Ovarian cancer



E

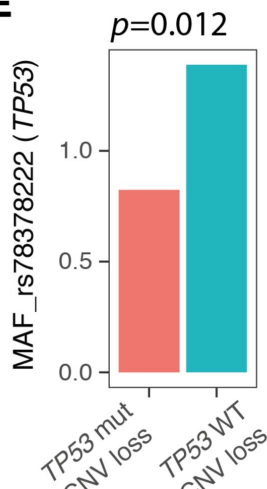


Figure 2

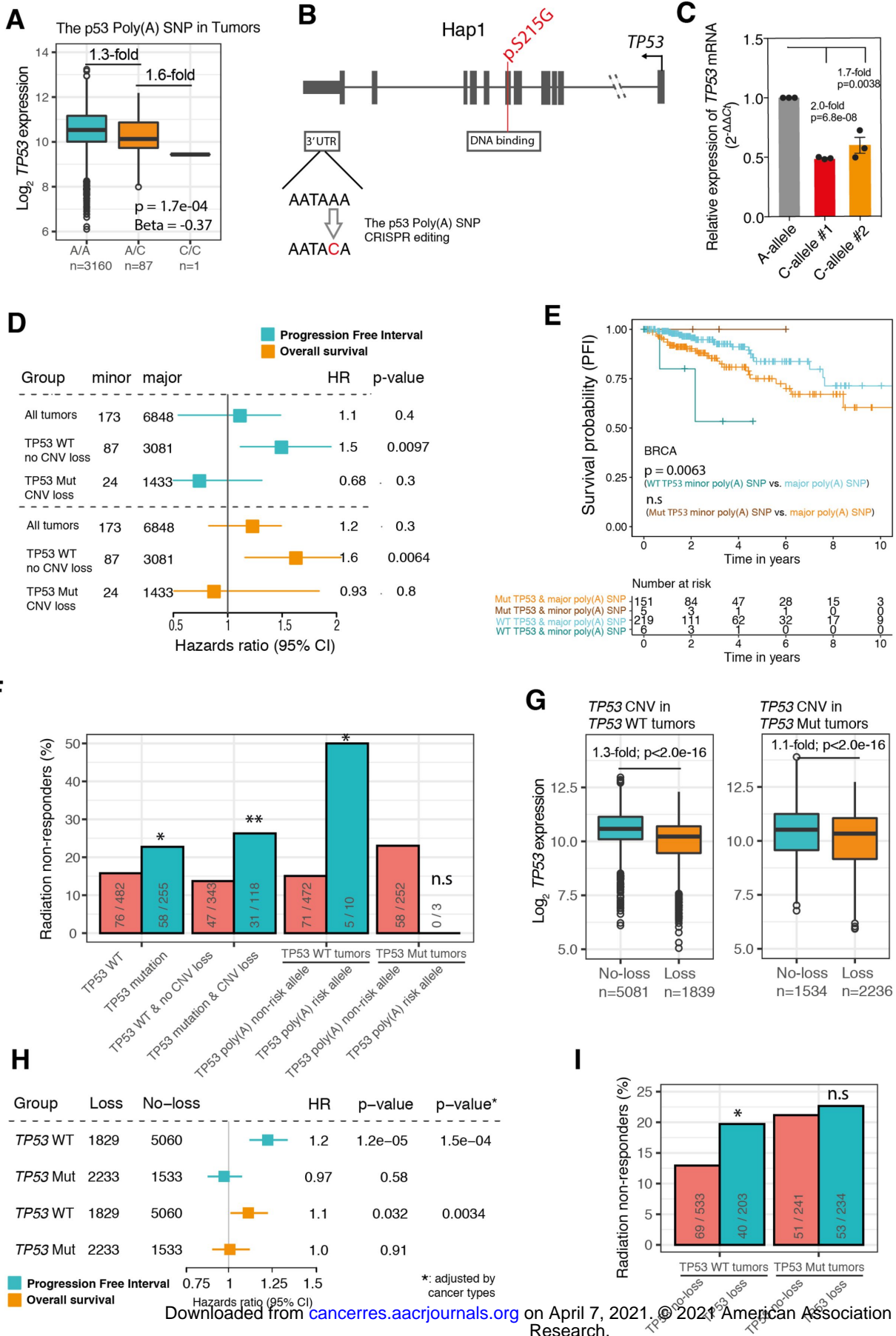


Figure 4

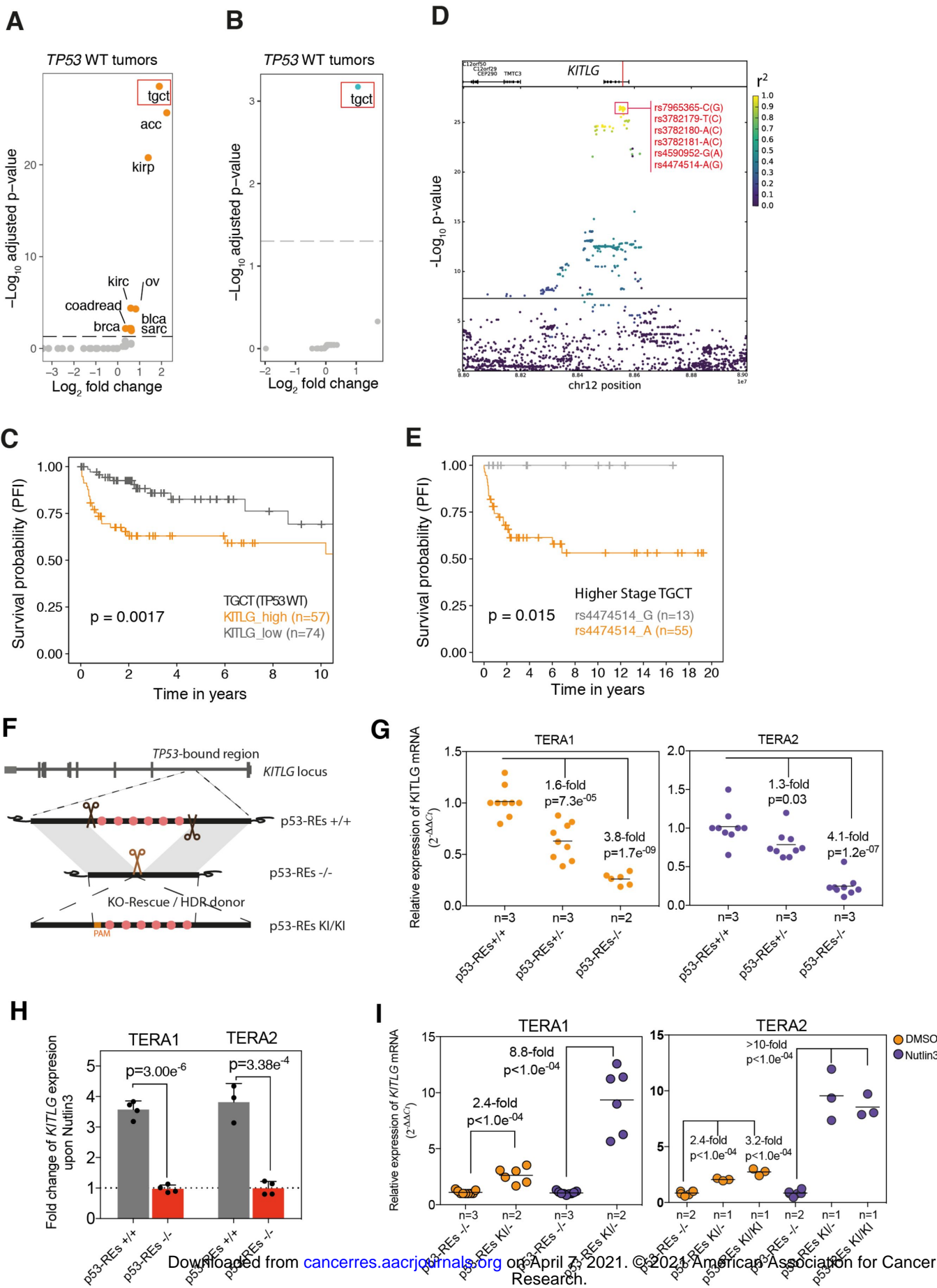


Figure 5

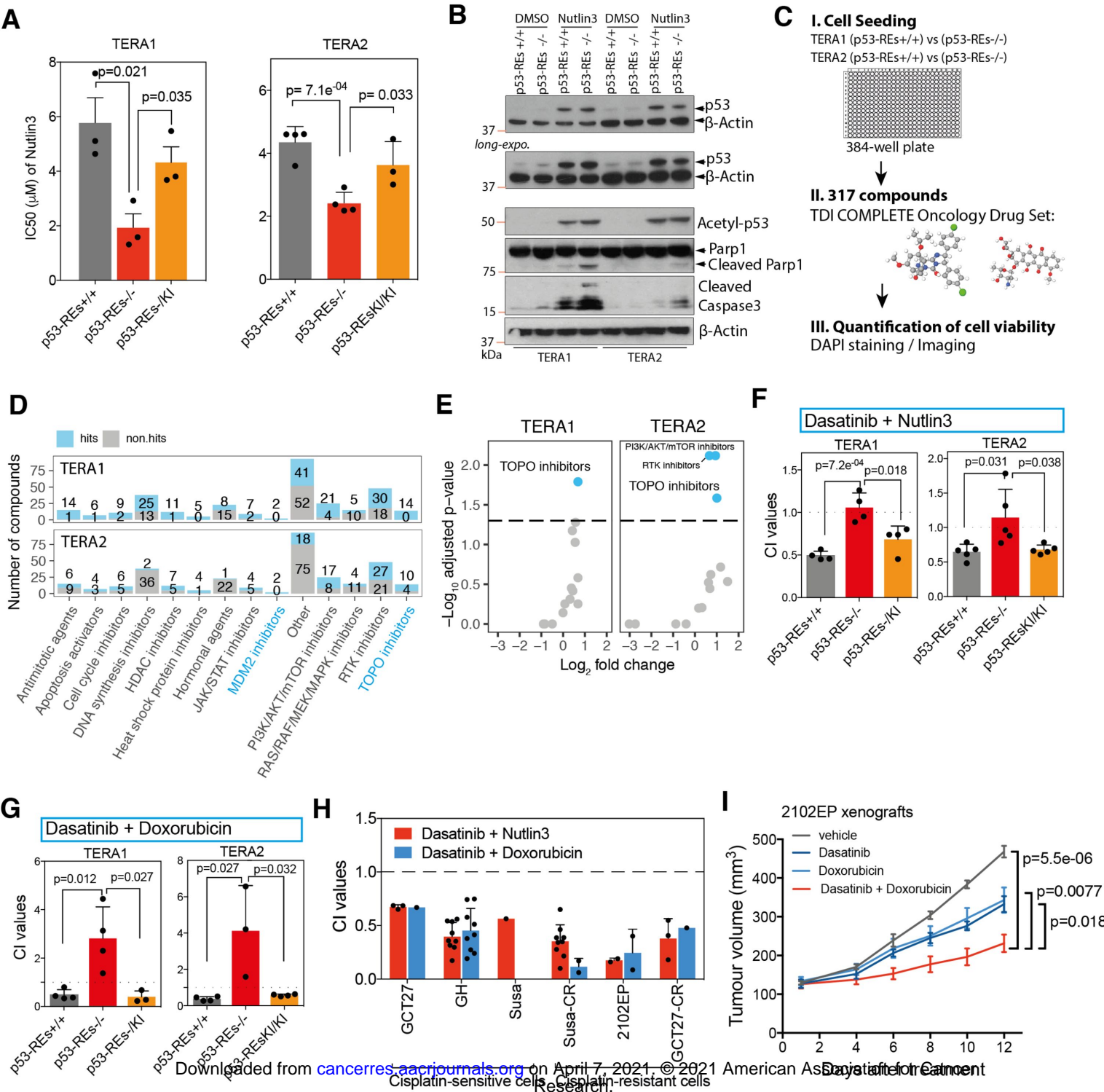
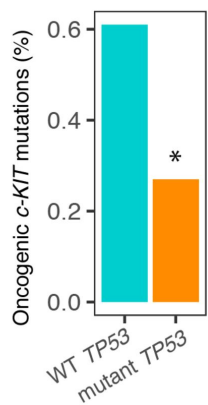
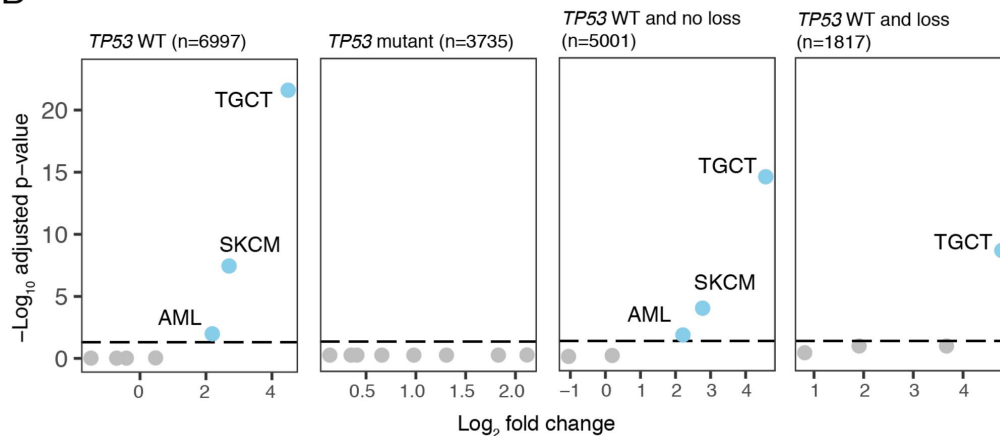


Figure 6

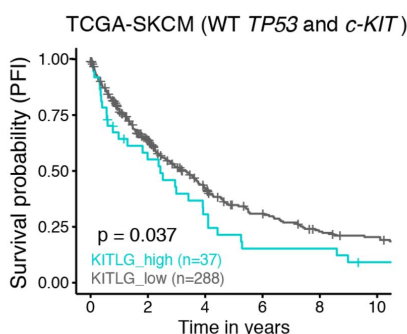
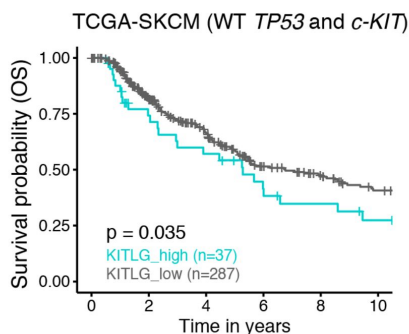
A



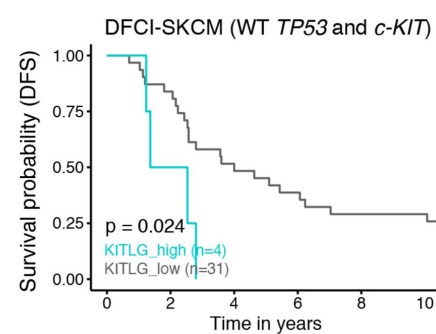
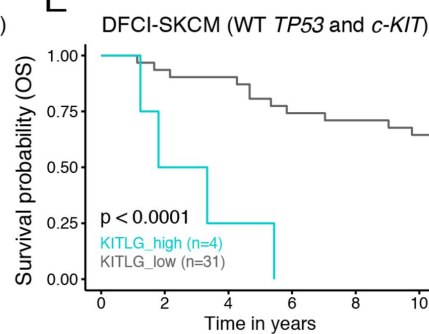
B



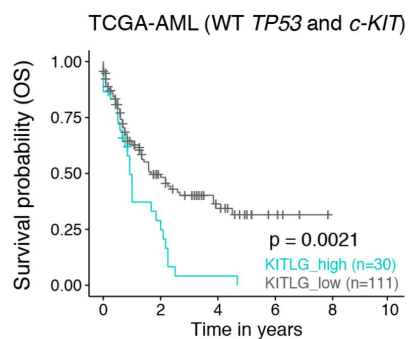
C



E



D



F

TCGA-SKCM (WT *c-KIT*)

Group	KITLG_high	KITLG_low	HR	p-value
<i>wtTP53</i> -no.loss	65	118	1.69	0.014 *
mutant <i>TP53</i> or <i>wtTP53</i> -loss	114	33	1.47	0.20
<i>wtTP53</i> -no.loss	65	119	1.41	0.047 *
mutant <i>TP53</i> or <i>wtTP53</i> -loss	129	18	0.64	0.12

Hazard ratio (95% CI)

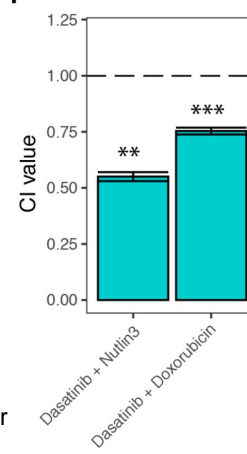
G

TCGA-AML (WT *c-KIT*)

Group	KITLG_high	KITLG_low	HR	p-value
<i>wtTP53</i> -no.loss	29	102	2.06	0.0031 *
mutant <i>TP53</i> or <i>wtTP53</i> -loss	7	12	0.51	0.19

Hazard ratio (95% CI)

H



Cancer Research

The Journal of Cancer Research (1916–1930) | The American Journal of Cancer (1931–1940)

Germline and somatic genetic variants in the p53 pathway interact to affect cancer risk, progression, and drug response

Ping Zhang, Isaac Kitchen-Smith, Lingyun Xiong, et al.

Cancer Res Published OnlineFirst February 8, 2021.

Updated version	Access the most recent version of this article at: doi: 10.1158/0008-5472.CAN-20-0177
Supplementary Material	Access the most recent supplemental material at: http://cancerres.aacrjournals.org/content/suppl/2021/02/05/0008-5472.CAN-20-0177.DC1
Author Manuscript	Author manuscripts have been peer reviewed and accepted for publication but have not yet been edited.

E-mail alerts	Sign up to receive free email-alerts related to this article or journal.
Reprints and Subscriptions	To order reprints of this article or to subscribe to the journal, contact the AACR Publications Department at pubs@aacr.org .
Permissions	To request permission to re-use all or part of this article, use this link http://cancerres.aacrjournals.org/content/early/2021/02/05/0008-5472.CAN-20-0177 . Click on "Request Permissions" which will take you to the Copyright Clearance Center's (CCC) Rightslink site.